Journal of Banking and Finance 108 (2019) 105654

Contents lists available at ScienceDirect

Journal of Banking and Finance

journal homepage: www.elsevier.com/locate/jbf

Volatility tail risk under fractionality☆

Giacomo Morelli[a,*], Paolo Santucci de Magistris[a,b]

[a] Department of Economics and Finance, LUISS University, Viale Romania 32, Roma 00197, Italy
[b] CREATES, Aarhus University, Fuglesangs Alle 4, Aarhus 8210, Denmark

ARTICLE INFO

Article history:
Received 7 July 2019
Accepted 19 September 2019
Available online 20 September 2019

JEL classification:
C01
C02
C58
G12
G13

Keywords:
Fractional Ornstein–Uhlenbeck
Supremum
Rough volatility
VIX
VolaR

ABSTRACT

We study the probabilistic properties of the fractional Ornstein–Uhlenbeck process, which is a relevant framework for volatility modeling in continuous time. First, we compute an expression for its variance for any value of the Hurst parameter, $H \in (0, 1)$. Second, we derive the density of the process and we calculate the probability of its supremum to be above a given threshold. We provide a number of illustrations based on fractional stochastic volatility models, such as those of Comte and Renault (1998), Bayer et al. (2016) and Gatheral et al. (2018). Finally, the empirical analysis, based on the realized variance series of S&P500, shows the usefulness of these theoretical results for risk management purposes, especially when a characterization of the volatility tail risk is needed.

© 2019 Elsevier B.V. All rights reserved.

1. Introduction

The volatility of asset returns is a key ingredient in a number of financial applications, including option pricing and risk management. Therefore, a proper characterization of its probabilistic properties is at the core of any well posed analysis of financial risks. In this paper, we provide expressions for the variance and the distribution of a class of fractional mean reverting processes, which are popular modeling frameworks for the dynamics of volatility of financial assets, see Comte and Renault (1998) and Gatheral et al. (2018) among others. We also derive an expression for the probability of their supremum being larger than a given threshold. This turns out to be of potential relevance in risk management applications, when the goal is to assign a probability to extremely high volatility events based on a precise characterization of the decay of the right tail of the volatility density.

The phenomenon of mean-reversion has been widely documented for both financial time-series, such as interest rates and volatility, and for macroeconomic aggregates, e.g. inflation. In empirical finance, Tan (1997) proposes mean-reverting principal component analysis for portfolio optimization to manage beta against alpha and Engle and Patton (2001) detect mean reversion in stocks' volatility. Filipovic (2007) finds evidence of mean reversion in energy stocks while Avellaneda and Lee (2010) study a statistical arbitrage strategy in U.S. equities driven by a mean reverting model that represents an effective barometer to monitor real-time risks and opportunities. From the methodological point of view, Vasicek (1977) is the first one to propose a continuous-time model allowing for mean reversion in interest rates. Subsequently, Cox et al. (1985) eliminate the main drawback of the Vasicek model, that is a non-null probability of negative values. Hull and White (1990) introduce time-inhomogeneous extensions capable of fitting any given initial forward rate curve and similar extensions for short rate models are in Bjork and Hyll (2000) and

☆ This paper combines material contained in Chapter 1 of Morelli's Ph.D. dissertation at Sapienza University. We are grateful to the Editor, Carol Alexander, and two anonymous referees for very helpful remarks and suggestions that improved the overall quality of this work. We also thank Andrea Barletta, Mikkel Bennedsen, Sara Biagini, Christian Brownlees, Filippo Ippolito, Eva Lütkebohmert-Holtz, Eulalia Nualart, Mikko Pakkanen, Alessio Sancetta, Marco Scarsini for their relevant remarks on our work. We would also like to thank seminar participants at the BGSE-Universitat Pompeu Fabra (Barcelona, 2014), La Sapienza University (Rome, 2014), LUISS (Rome, 2019), Freiburg University (Freiburg, 2019), 30th Jerusalem Advanced School of Economics (Jerusalem, 2019). Paolo Santucci de Magistris gratefully acknowledges the research support of the Project 2 grant of the Danish Council for Independent Research (IRFD), Social Sciences, number 8019-00015A, the research support of AUFF and CREATES, funded by the Danish National Research Foundation, Denmark (DNRF78).

* Corresponding author.
E-mail addresses: morellig@luiss.it (G. Morelli), sdemagistris@luiss.it (P. Santucci de Magistris).

https://doi.org/10.1016/j.jbankfin.2019.105654
0378-4266/© 2019 Elsevier B.V. All rights reserved.

Brigo and Mercurio (2001). More recently, Kwona (2007) introduces an extension of time-inhomogeneous affine term structure models with mean-reversion in the level. Applications, other than to interest rates, are to stochastic models that describe the mean reverting behavior of volatility, see Heston (1993), and of volatility of volatility, see Kaeck and Alexander (2013). On the other hand, a striking evidence emerging from the analysis of observable quantities such as the realized variance, formally defined by Barndorff-Nielsen and Shephard (2002a,b), is that the volatility of stock returns, although being a mean-reverting process, is characterized by long-range dependence or long-memory. For instance, Andersen et al. (2001a) and Andersen et al. (2003) report evidence of stationary long memory in the realized variance series. The same type of long range dependence is found in time series of interest rates (Lai, 2004) and exchange rates (Andersen et al., 2001b). This empirical evidence challenges the classical framework for the analysis of mean-reverting processes, which is based on a diffusive component driven by the standard Brownian motion.

To comply with the empirical evidence of long-memory in volatility, Comte and Renault (1998) propose a version of the Ornstein–Uhlenbeck (OU henceforth) process for the logarithm of the instantaneous variance, where the innovations are driven by the fractional Brownian motion introduced by Kolmogorov (1940) and further analyzed in Mandelbrot and Van Ness (1968). The dynamic properties of the innovations of the fractional Brownian motion are defined is terms of the so-called Hurst exponent, H, which is bounded between 0 and 1. Comte and Renault (1998) find that long-memory in volatility is consistent with a value of the H parameter above 0.5. As in Gatheral et al. (2018), we name this model fractional stochastic volatility (FSV) model. More recently, Rossi and Santucci de Magistris (2014) have shown that the integrated variance, and hence also realized variance, inherit the same degree of fractional integration as the instantaneous variance generated by the FSV model. A recent strand of the literature, see Gatheral et al. (2018), has shown empirical evidence that volatility models should incorporate a roughness term (irregular behavior at short time scales), which is associated with a fractional Brownian motion with Hurst exponent smaller than 0.5. This entails that the innovations to the log-variance are antipersistent, from which the notion of *rough* volatility. For this reason, Gatheral et al. (2018) name their model *rough* fractional stochastic volatility (RFSV). An alternative version of the fractional OU process has been recently adopted in Bayer et al. (2016) with the purpose of pricing VIX options under the constraint of rough stochastic volatility.

Despite the evident appeal of continuous-time stochastic models driven by the fractional Brownian motion, probability density functions and probability of the supremum for these type of mean reverting processes have not been investigated yet in literature. The contribution of this paper is to derive the distribution of fractional mean reverting processes and of their supremum. Earlier results about the limiting distribution of the supremum of a sequence of random variables are in Gnedenko (1943). Recently, Embrechts and Puccetti (2006a),Embrechts and Puccetti (2006b) provide bounds on the distribution function of the sum of risks, when no information on the structure of dependence of the random vector is available. Bounds on risk measures for risk aggregation with dependence uncertainty are studied in Bernard et al. (2014) and Bernard and Vanduffel (2015), whereas a theoretical foundation for the measurement of tail risk is provided in Kou and Peng (2016). A main task in risk management is to look for bounds for the financial variables constituting the portfolio with primary interest in managing risk levels within defined tolerance thresholds without being over controlled or forgoing desirable opportunities. For instance, Chen and Tu (2013) computes the Value-at-risk (VaR) of an hedged portfolio with a mix of fixed and floating rate debt for which bounds on the underlying yield rates are of crucial importance.

Our theoretical findings are based on the fractional version of the OU process, fOU henceforth, which encompasses both the FSV and the RFSV models in the stochastic volatility context. In particular, in Proposition 1 we provide an expression for the variance of the fOU for any value of $H \in (0, 1)$. We use this result to derive the density of the fOU process in Lemma 1. Furthermore, we adapt the results of Nourdin (2012) to the fOU context providing the probability of the supremum of the fOU being larger than a given threshold (Proposition 2). We outline a number of examples to illustrate our theoretical results. The examples are based on the FSV and RFSV specifications, where for the latter the parameters are calibrated on the S&P 500 volatility series under the restriction of Hurst parameter below 1/2. Furthermore, we also extend Proposition 2 to the case of the rough Bergomi model by Bayer et al. (2016), which leads to the derivation of the probability of the supremum in the context of VIX options. Finally, we empirically illustrate the usefulness of our theoretical results for risk management purposes and we estimate the parameters of the fOU process by indirect inference based on the time series of the RV of SPX and we compute the density of the daily volatility. Given this density, we can compute relevant quantities like the *Volatility-at-risk*, that is the analogous of the VaR in the volatility context.

The paper is organized as follows. After a brief description of the fOU process, Section 2 provides the theoretical background of this paper, with examples based on well known stochastic volatility models under fractionality. Subsequently, Section 3 reports the findings of the empirical analysis of the fOU process in the context of stochastic volatility modeling and tail volatility risk. Finally, Section 4 concludes.

2. Theoretical background

Here and throughout the paper every random object is defined on the appropriate probability space $(\Omega, \mathcal{F}, \mathbb{P})$. The (one-dimensional) fOU process $X^H = \{X^H(t), t \geq 0\}$ driven by the fractional Brownian motion is the solution to the SDE

$$dX^H(t) = a\big(t, X^H(t)\big)dt + b\big(t, X^H(t)\big)dB^H(t), \quad t > 0,$$
$$X_0^H = x_0, \tag{1}$$

where $a(t, X^H(t))$ and $b(t, X^H(t)) \neq 0$ are real-valued functions assumed to posses derivatives and $B^H(t)$ is a standard fractional Brownian motion with Hurst parameter $H \in (0, 1)$, see for an introduction (Mandelbrot and Van Ness, 1968). In the case with $b\big(t, X^H(t)\big) = \eta$ constant and $a\big(t, X^H(t)\big) = \theta\big(m - X^H(t)\big)$ with the speed of mean reversion parameter $\theta > 0$, and m real number. The solution of Eq. (1) starting at $X^H(0) = x(0)$ is

$$X^H(t) = m + x_0 e^{-\theta t} + \eta e^{-\theta t} \int_0^t e^{\theta s} dB^H(s), \tag{2}$$

where the mean of the process in (2) is $\mu(t) := \mathbb{E}[X^H(t)] = m + x_0 e^{-\theta t}$, see Cheridito et al. (2003). The following proposition provides an explicit formula for the variance of the fOU.

Proposition 1 (Variance of fOU)**.** *Let $X^H(t)$ be a fOU process as in (2) for $H \in (0, 1)$. Then, the variance of $X(t)^H$ is*

$$\mathbb{V}ar[X^H(t)] = \eta^2 t^{2H} - \theta\eta^2 e^{-\theta t} \int_0^t e^{\theta u}(t^{2H} + u^{2H} - |t-u|^{2H})du$$
$$+ \theta^2\eta^2 e^{-2\theta t} \frac{1}{2} \int_0^t \int_0^t e^{\theta u} e^{\theta v}(u^{2H} + v^{2H} - |u-v|^{2H})dudv. \tag{3}$$

Proof. The proof is in Appendix A. □

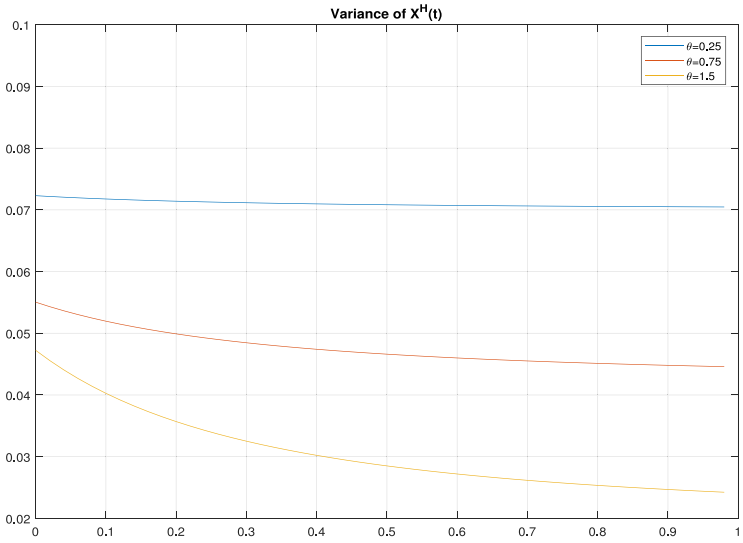

Fig. 1. Variance of fOU. The plot reports the variance of $X^H(t)$ as a function of $H \in [0.0001, 0.9999]$ (x-axis), when $X^H(t)$ follows the fOU process with different values of $\theta = [0.01, 0.75, 1.5]$. The other parameters of the model are $\eta = 0.3$ and $m = -5$.

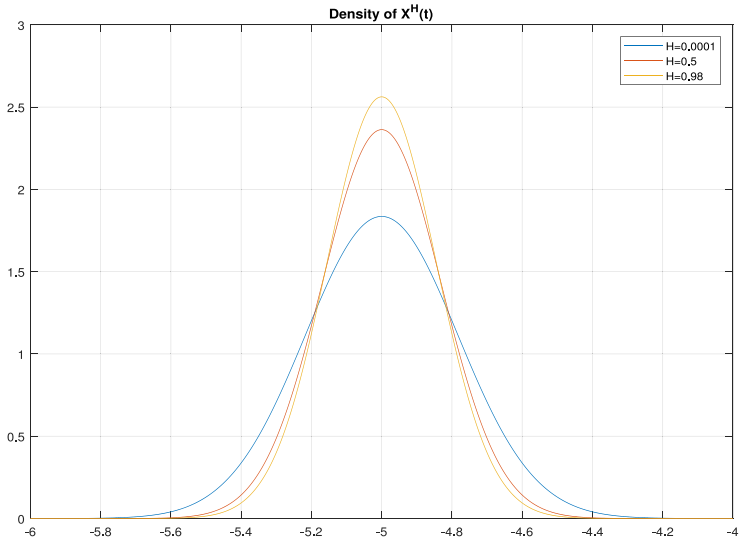

Fig. 2. Density of fOU. The plot reports the density of $X^H(t)$ when the latter follows the fOU process with different values of $H = [0.0001, 0.5, 0.98]$. The other parameters of the model are $\eta = 0.3$, $\mu = -5$ and $\theta = 1.5$.

Fig. 1 plots the variance of X_t^H as a function of H, showing that the variance of the fOU is inversely related with H. Notably, the integrals in (3) are not available in closed form and need to be computed by numerical integration.[1] Furthermore, the variance decreases with the speed of mean reversion, being close to the variance of a fractional Brownian motion for $\theta \approx 0$.

Proposition 1 allows us to explicitly derive the probability distribution function of the fOU process.

Lemma 1. *(Density of fOU process) Let $X^H(t)$ be a fOU process as in (2). Then $X^H(t) \sim \mathcal{N}(\mu(t), \varsigma(t))$, with $\mu(t) := \mathbb{E}[X^H(t)] = m + x_0 e^{-\theta t}$ and $\varsigma(t) := \mathbb{V}ar[X^H(t)]$.*

Proof. The fOU process is a linear combination of a Gaussian processes - the fractional Brownian motion - and it is therefore Gaussian. The mean $\mu(t) = m + x_0 e^{-\theta t}$ is readily checked, and the variance $\varsigma(t) := \mathbb{V}ar[X^H(t)]$ is computed in Proposition 1. □

Fig. 2 shows the density of $X^H(t)$ computed for different values of the Hurst parameter, H. The figure highlights the Gaussian shape of the density of $X^H(t)$ as well as the decreasing variance as H increases.

2.1. Supremum of the fOU process

We now turn the attention to the asymptotic behavior of the supremum of the fOU process.

Proposition 2 (Distribution of the supremum of the fOU process)**.** *Let $X^H = \{X^H(t), t \in [0, 1]\}$ be a fOU process on the interval [0,1]. Define $M^H = \sup X^H$ be the supremum of $X^H(t)$ on the interval [0,1]. It follows that*

$$\lim_{x \to \infty} \mathbb{P}(M^H \geq x) = \exp\left(-\frac{x^2}{2\mathbb{V}ar[X^H(1)]}\right).$$

Proof. The proof is in Appendix B. □

[1] We adopt the MATLAB command `int(·)` that uses the quadrature method to evaluate the integral. This is a more accurate alternative than the trapezoidal method studied in Delves and Lyness (1967).

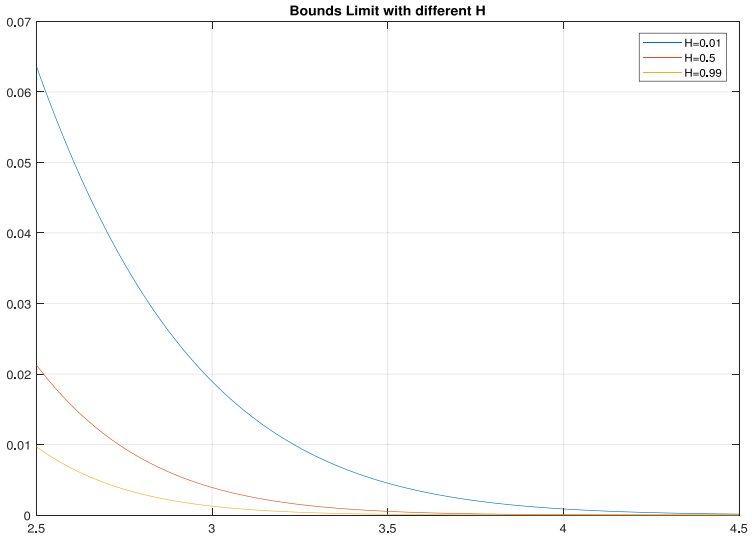

Fig. 3. Probability of the supremum of the fOU process. The plot reports the tail probability of $M^H = \sup X^H$, when X^H follows the fOU process with different values of $H = [0.01, 0.5, 0.99]$. The other parameters of the model are $\eta = 1.5$, $\mu = -5$ and $\theta = 0.3$.

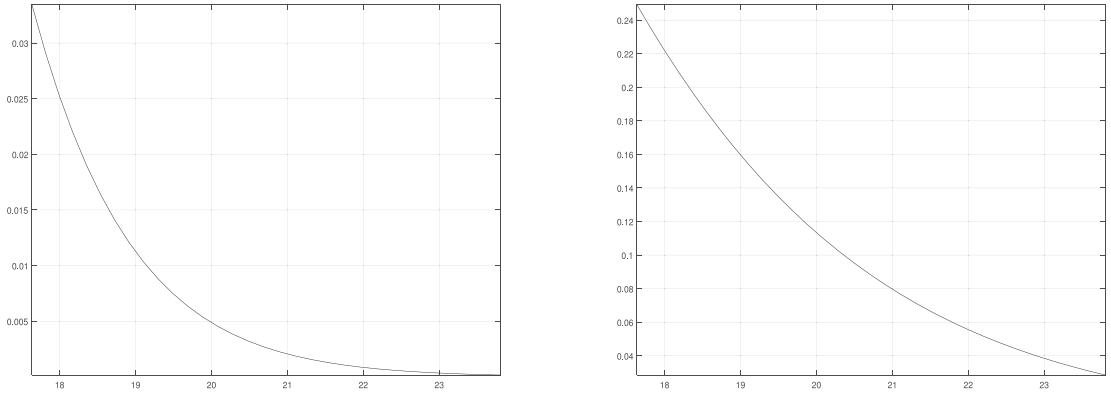

(a) FSV (b) RFSV

Fig. 4. Probability of the supremum of FSV and RFSV model. The plot reports the tail probability of $M^H(t) = \sup \sigma(t)$, when $\log \sigma(t)$ follows the FSV (Panel a) and the RFSV (Panel b) processes with parameter values calibrated as in Comte and Renault (1998) and Gatheral et al. (2018). The parameters of the RFSV model are $\nu = 0.3$, $m = -5$ and $\kappa = 1$, $H = 0.8$. The parameters of the RFSV model are $\nu = 0.3$, $m = -5$ and $\kappa = 5 \times 10^{-4}$, $H = 0.14$. On the x-axis volatility is expressed in annualized percentage terms.

Proposition 2 derives the probability of the supremum of the fOU process as an explicit function of its variance computed in Proposition 1. Such limit is reported in Fig. 3 for changing values of the quantile x on the right tail. The figure shows that, ceteris paribus, the smaller the H, the higher the probability associated to events on the right tail.

As an illustration, we consider the modeling framework adopted both in Comte and Renault (1998) and Gatheral et al. (2018), who propose the FSV and RFSV models respectively. Specifically, the volatility is modeled as

$$\sigma(t) = \exp Y^H(t), \quad t > 0$$

where $Y^H(t)$ is a fOU process satisfying

$$dY^H(t) = \kappa\left(m - Y^H(t)\right)dt + \nu dW^H(t), \tag{4}$$

$m \in \mathbb{R}$, ν and κ are positive parameters and $W^H(t)$ denotes the fractional Brownian motion of Hurst parameter $H > 1/2$ (FSV) and $H < 1/2$ (RFSV). Fig. 4 shows the probability of the supremum of the FSV model and of the RFSV model. The parameters are calibrated according to those reported in Comte and Renault (1998) and Gatheral et al. (2018), which are based on S&P 500 volatility series. In particular, in Comte and Renault (1998) $H > 1/2$ and $\theta \gg 0$, meaning that the speed of mean reversion is rather strong but the innovations to the (log) volatility are persistent. Instead, in the setting of Gatheral et al. (2018), $H < 1/2$ but $\kappa \ll 1/T$, that is $\kappa = 0.0005$. In the context of RFSV the variance of Y_t^H can be approximated with that of the fractional Brownian motion, that is $\mathbb{V}ar[Y^H(t)] \approx \nu^2 t^{2H}$, see Bayer et al. (2016, p.899). In other words, the trajectory of volatility are mostly governed by the fractional Brownian motion, which is associated with antipersistent innovations when $H < 1/2$. In particular, the value of H in the RFSV is 0.14, while the speed of mean reversion, κ, is tight to zero, thus signaling an almost absent role of the mean reverting term, which is in line with the findings in Rossi and Santucci de Magistris (2014). With this setup, the probability that the supremum of volatility is above 22% on annual basis is 5.6%, while the same probability reduces to 0.09% when adopting the FSV. This difference is due to the more erratic (rough) behavior of volatility in the RFSV model, rather than in the FSV specification.

Finally, Fig. 5 shows the density of $\sigma(t)$ for both the FSV and RFSV models. The density is lognormal in both cases, as a consequence of Proposition 1. The distribution of FSV is more concen-

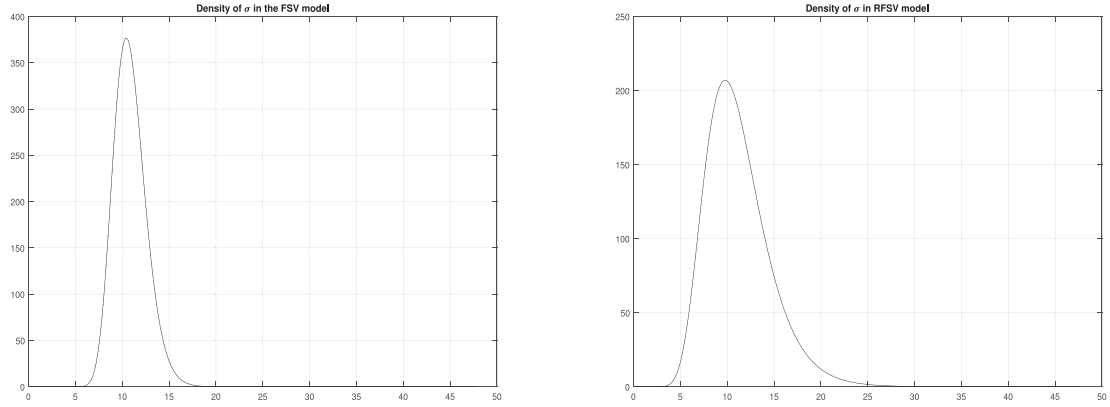

(a) FSV (b) RFSV

Fig. 5. Density of $\sigma(t)$. The plot reports the density of $\sigma(t) = \exp X^H(t)$, when $X^H(t)$ follows the fOU process. The parameters of the RFSV model are $\nu = 0.3$, $m = -5$ and $\kappa = 1$, $H = 0.8$. The parameters of the RFSV model are $\nu = 0.3$, $m = -5$ and $\kappa = 5 \times 10^{-4}$, $H = 0.14$. On the x-axis volatility is expressed in annualized percentage terms.

trated around the mean, and it gives a probability of 1.55% to the event that $\sigma(t)$ is above 15% on an annual basis. On the contrary, the density of $\sigma(t)$ in the RFSV case is more dispersed and it assigns a probability of 12.6% to the same event.

2.1.1. Supremum in the rBergomi model

The range of applicability of Proposition 2 extends beyond the fOU framework. Therefore, as a further application of Proposition 2, we compute the probability of the supremum of the square VIX following the rough volatility model studied in Bayer et al. (2016). VIX measures the one-month ahead risk-neutral market expectation of the level of volatility of S&P 500 index and it is often referred to as the *fear* index. Thus, being able to compute the distribution for the supremum of the (square) VIX might be relevant for risk management purposes. Bayer et al. (2016) exploit the rough volatility model of Gatheral et al. (2018) as option pricing model. In particular, they introduce a generalization of the model of Bergomi (2005), which they refer to as rough Bergomi (rBergomi), see also Jacquier et al. (2018) and Sauri (2019). In the rBergomi framework, the instantaneous variance is modeled as

$$v(t) = v_0 \exp\left(Z(t) - \frac{\psi^2}{2} t^{2\vartheta+1}\right), \quad v_0 > 0, t > 0 \tag{5}$$

where ψ is a positive parameter, $\vartheta \in (-1/2, 0)$ and Z is a Holmgren-Riemann-Liouville fractional Brownian motion defined by

$$Z(t) = \int_0^t K_\vartheta(s,t) dW(s), \quad \text{for any } t \geq 0, \tag{6}$$

with $W(t)$ standard Brownian motion and the integrand

$$K_\vartheta(s,t) = \psi\sqrt{2\vartheta+1}(t-s)^\vartheta, \quad \text{for any } 0 \leq s < t.$$

We follow Bayer et al. (2016, p. 888) in that the instantaneous variance defined in (5) is equivalent to the one generated by the rough fOU process as in Gatheral et al. (2018). Model calibration is achieved in Bayer et al. (2016) by examining the term structure of VIX options. We denote the terminal value of the VIX futures by $\sqrt{\zeta(T)}$ and its square

$$\zeta(T) = \frac{1}{\tau}\int_t^T \mathbb{E}[v(u)|\mathcal{F}(t)]du, \tag{7}$$

where $\tau = T - t$. Bayer et al. (2016) obtain an approximation of the variance of $\log\sqrt{\zeta(T)}$ conditional on $\mathcal{F}(t)$, that is

$$\mathbb{V}ar[\log\sqrt{\zeta(T)}|\mathcal{F}(t)] \approx \frac{1}{4}\psi^2(\tau)^{2H} f^H\left(\frac{1}{1-t}\right), \tag{8}$$

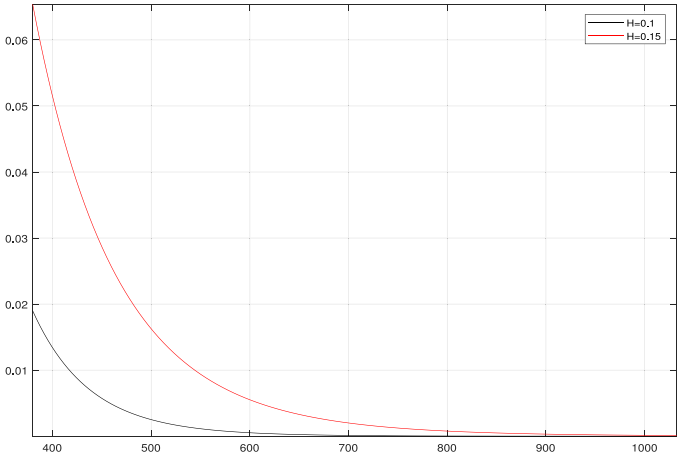

Fig. 6. Probability of the supremum of the square VIX in the rBergomi model. The plot reports the tail probability of $M^\zeta = \sup\log\zeta(t)$, where $\zeta(t)$ is given by the rBergomi model as in Bayer et al. (2016) for different values of H. The parameters of the model are $\psi = 3.5$, $v_0 = -10$ and $\vartheta = 5 \times 10^{-4}$, $H = 0.10, 0.15$. On the x-axis is expressed in the square VIX scale and it is in annualized percentage terms.

where $\mathbb{V}ar[\log\sqrt{\zeta(T)}|\mathcal{F}(t)]$ is nothing else that the square of the VVIX index for a τ horizon. The following lemma provides the distribution of the supremum of $\log\zeta(t)$ in the rBergomi model.

Lemma 2 (Supremum of the log-square VIX in the rBergomi model)**.** *Let $v(t)$ follow the rBergomi model in (5). Let $\zeta = \{\zeta(t), t \in [0,1]\}$ denote value of the square VIX futures as defined in (7). Define $M^\zeta = \sup\log\zeta$ the supremum of the log-square VIX, then*

$$\lim_{x\to\infty} \mathbb{P}(M^\zeta \geq x) = \exp\left(-\frac{x^2}{2\psi^2(1-t)^{2H} f^H\left(\frac{1}{1-t}\right)}\right),$$

where $f^H\left(\frac{1}{1-t}\right) = D_H^2(1-t)\int_0^1\left[\left(\frac{2-t}{1-t}-x\right)^{1/2+H} - (1-x)^{1/2+H}\right]^2 dx$, *with* $D_H = \frac{\sqrt{2H}}{H+1/2}$.

Proof. As noted by Bayer et al. (2016, p.895), the VIX payoff and its square $\zeta(T)$ are log-normally distributed. Hence proof of Proposition 2 applies to the process $\{\log\zeta(t),\ t \in [0,1]\}$. The expression for the variance of $\log\zeta(t)$ is derived in Bayer et al. (2016, p.896), that is $\mathbb{V}ar[\log\zeta(T)|\mathcal{F}(t)] = \psi^2(1-t)^{2H} f^H\left(\frac{1}{1-t}\right)$. □

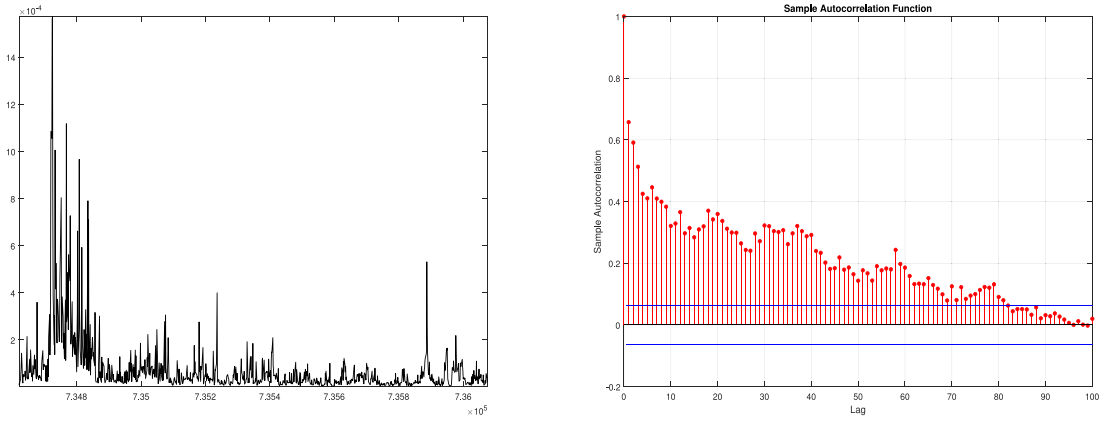

(a) RV (b) ACF

Fig. 7. Time series of *RV* of S&P 500 based on sampling log-returns over 5 minutes intervals and its ACF.

As an illustration, Fig. 6 reports the probability of the supremum of the log-square VIX in the rBergomi model, when the parameters are calibrated according to those reported in Bayer et al. (2016), which are based on VIX series. The figure shows that the probability of the supremum is an increasing function of H. For instance, with $H = 0.10$ the rBergomi model assigns a probability of 1.3% to the event of the supremum of the square VIX being larger than 400, while the same probability increases to 5% when $H = 0.15$. Given that the highest daily level of VIX ever recorded was 89.53% on October 24, 2008, the rBergomi model assigns an infinitesimal probability to the event of the supremum of VIX being above this threshold.

3. Empirical analysis

3.1. Density of the fOU volatility model

The theoretical results presented in Section 2 are applied to the fractional stochastic volatility (FSV) process, see Comte and Renault (1998). We consider the following FSV

$$\begin{aligned} \frac{dS(t)}{S(t)} &= \mu(t)dt + \sigma(t)dW(t) \\ \sigma(t) &= \exp X^H(t) \\ dX^H(t) &= \theta\big(m - X^H(t)\big)dt + \eta dB^H(t), \quad t > 0 \end{aligned} \tag{9}$$

where $S(t)$ is the underlying asset price, $\mu(t)$ is a suitable drift term in price, $W(t)$ is a standard Brownian motion possibly correlated with $B^H(t)$, $\sigma(t)$ is the volatility process, and $X^H(t)$ follows a fOU process.

We now provide an empirical illustration of the theoretical results presented in Sections 2 and 2.1 based on the stochastic volatility model in (9). We estimate the parameters of the SV model in (9) based on intradaily returns, $r_{t,l}$, [2] of S&P 500 from April 28, 2011 to April 21, 2015, for a total of $T = 1000$ day. The time series of $RV_t = \sum_{l=1}^{L} r_{t,l}^2$ is computed with returns sampled at 5-minute frequencies, that is $l = 1, \dots, L$ with $L = 78$. Liu et al. (2015) find limited empirical support that the 5-minute *RV* is outperformed by other (more refined) measures of integrated variance. Furthermore, we can consider 5- minute *RV* not to be contaminated by the market microstructure noise features, such as bid-ask bounce and decimalization effects. The dynamics of the *RV* series is reported in Fig. 7 together with its sample autocorrelation function (ACF). The *RV* series displays the changing regime of volatility, where the latter reaches high levels towards the end of 2011 due to the sovereign debt crisis in Europe, and it is relatively low during the rest of the period. This switching behavior leads to high persistence as it is emphasized by the slow decay rate of the ACFs, and it is consistent with long memory in volatility as measured by values of $H > 1/2$.

We estimate the parameters of model (9) by means of indirect inference, see Corsi and Renò (2012) and Rossi and Santucci de Magistris (2018). In particular, we simulate S trajectories of daily *RV* from the model in (9)[3] and we find the $p \times 1$vector of parameters $\zeta = [\theta, m, \eta, H]'$, which minimizes the following criterion function $\Xi_T(\zeta)$, that is

$$\hat{\zeta}_{ST} = \arg\min_{\zeta} \Xi_T(\zeta) = \arg\min_{\zeta} (\hat{\beta}_T - \hat{\beta}_{ST}(\zeta))' \Omega_T (\hat{\beta}_T - \hat{\beta}_{ST}(\zeta)) \tag{10}$$

with $\hat{\beta}_{ST}(\zeta) = \frac{1}{S}\sum_{s=1}^{S} \hat{\beta}_T^s$ being the $q \times 1$ vector of estimates of the auxiliary model parameters based on the simulated paths, while $\hat{\beta}_T$ are the estimates of the auxiliary model parameters based on the observed sample. The matrix Ω_T is a weighting matrix, and it is chosen to maximize the asymptotic efficiency of the estimator $\hat{\zeta}_{ST}$. Under the set of assumptions outlined in Gouriéroux et al. (1993), $\hat{\zeta}_{ST}$ is consistent and asymptotically Gaussian. As auxiliary model, we chose the heterogeneous autoregression (HAR) of Corsi (2009),

$$RV_t^* = \gamma_0 + \gamma_1 \log RV_{t-1}^* + \gamma_2 \overline{RV}_{t-1,5}^* + \gamma_3 \overline{RV}_{t-1,10}^* + \gamma_4 \overline{RV}_{t-1,22}^* + \varepsilon_t, \tag{11}$$

where $RV_t^* = \log RV_t$, $\overline{RV}_{t-1,5}^* = \frac{1}{5}\sum_{i=1}^{5} \log RV_{t-1-i}^*$, $\overline{RV}_{t-1,10}^* = \frac{1}{10}\sum_{i=1}^{10} \log RV_{t-1-i}^*$ and $\overline{RV}_{t-1,22}^* = \frac{1}{22}\sum_{i=1}^{22} \log RV_{t-1-i}^*$ are the weekly, bi-weekly and monthly averages of $\log RV_t$. Notably, the HAR has a long autoregressive structure, that is an AR(22) with linear restrictions on the parameters, which mimics the long-memory features of $\log RV_t$. Furthermore, the HAR parameters, $\beta = [\gamma_0, \gamma_1, \gamma_2, \gamma_3, \gamma_4, \sigma_\varepsilon^2]'$, can be estimated by OLS. Hence, the HAR is a natural candidate to be a good auxiliary model in this context. Indeed, the long memory features generated by the fractional Brownian motion can be well approximated by the superposition of volatility factors, Corsi (2009), or by a stochastic volatility level parameter, as in Kaeck and Alexander (2012). Since the number of auxiliary parameters ($q = 6$) is larger than the number of structural parameters in ζ ($p = 4$), the weighting

[2] The subscript t denotes the observation day, and the subscript l denotes the intradaily period.

[3] The trajectories of the fractional Brownian motion are generated by fast Fourier transform, see Kroese and Botev (2015).

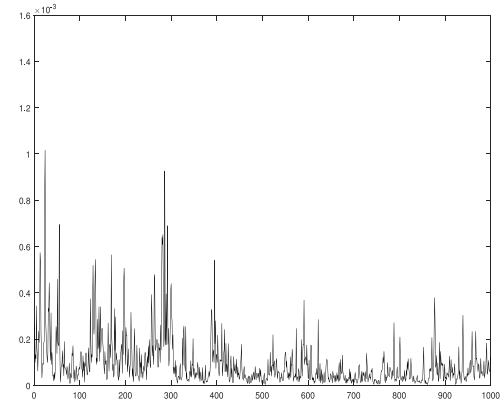

(a) Simulated RV - FSV

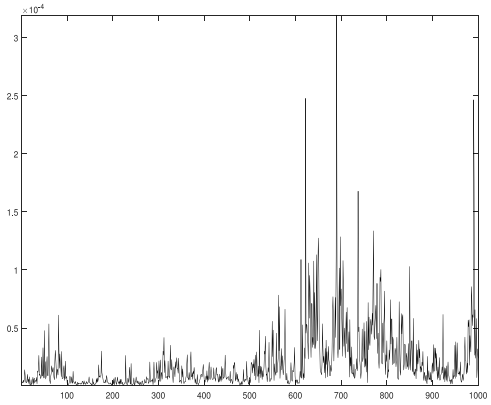

(b) Simulated RV - RFSV

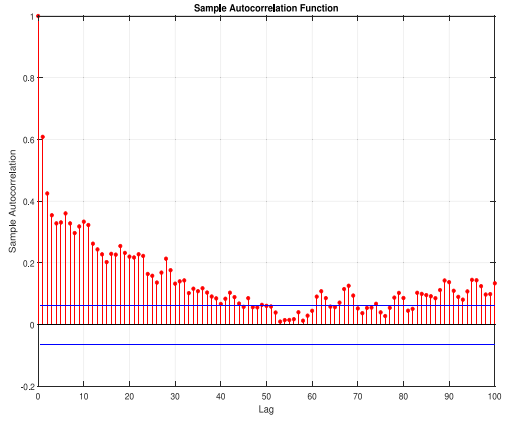

(c) ACF - FSV

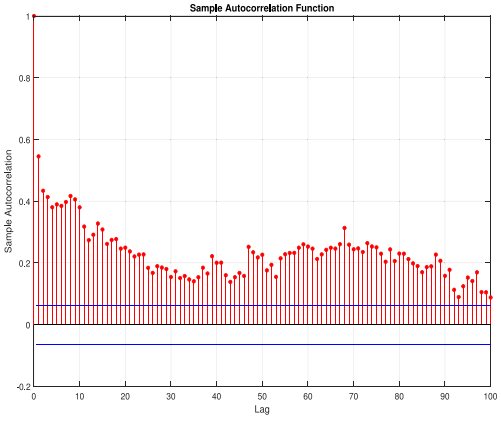

(d) ACF -RFSV

Fig. 8. Simulated time series of *RV* and its ACF for FSV and RFSV models.

Table 1
Parameter estimates by indirect inference. The left panel reports the estimates of the FSV model of Comte and Renault (1998). The right panel repots the estimates of the RFSV model of Gatheral et al. (2018).

	FSV				RFSV			
ζ	*Est.*	*Std.Err.*	$t-Stat$	$P-val$	*Est.*	*Std.Err.*	$t-Stat$	$P-val$
θ	9.9569	0.5104	19.5072	0.0000	0.0005	–	–	–
m	−5.2410	0.0026	−1985.16	0.0000	−5.5263	0.0330	−167.652	0.0000
η	0.9783	0.0496	19.7345	0.0000	7.4175	0.0234	316.399	0.0000
H	0.9276	0.0016	583.136	0.0000	0.0236	0.0002	102.444	0.0000

matrix Ω_T must be optimally chosen, and it is set as the inverse of the covariance matrix of the OLS estimates of β. The parameter estimates are reported in Table 1.

All parameters are strongly significant. The estimated value of H is close to the upper bound, while we have a strong mean-reversion effect as measured by the θ parameter estimated above 9.9. These parameter estimates are rather different from those of the RFSV model, which restrict the parameter H to be smaller than 0.5 (and around 0.14), but set the speed of mean-reversion very close to zero. This means that, with a negligible mean reversion term, the dynamics of $\sigma(t)$ are mostly governed by the fractional Brownian motion only with antipersistent innovations $H < 1/2$, see the discussion in Rossi and Santucci de Magistris (2014) and Bennedsen et al. (2016). Instead, with a strong mean-reversion effect the innovations to the volatility process can be persistent, that is $H > 1/2$. In other words, the innovation to the log volatility process are long memory, while the estimates of the long-mean are associated to an average value of daily volatility around 0.78%, that is 12.48% on an annual basis. Fig. 8 shows a simulated trajectory of *RV* based on the. The simulated *RV* series replicates the main features of the observed one, including the long-memory features as emerges also from the ACF.

Furthermore, the implied density of the volatility, $\sigma(t)$, is reported in Fig. 9 for the FSV. The long right tail of the distribution of $\sigma(t)$ assigns non-negligible probability to high-values of volatility. For instance, the probability that volatility is above 35% on annual basis is around 0.7% in the FSV model, and around 2.4% in the RFSV model. The FSV ad RFSV models allow us to estimate the volatility-at-risk, namely the VolaR see Caporin et al. (2017), that is the analogous of the value-at-risk (VaR) in the volatility context,

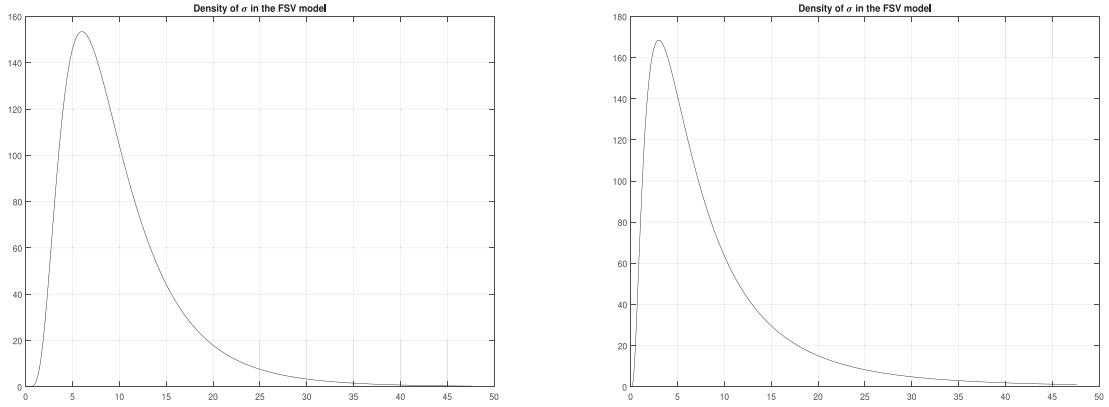

(a) FSV (b) RFSV

Fig. 9. Density of $\sigma(t)$ based on the estimates. The plot reports the density of $\sigma(t) = \exp X^H(t)$, when $X^H(t)$ follows the FSV and RFSV processes, respectively. On the x-axis volatility is expressed in annualized percentage terms.

i.e. the risk of extreme high volatility. In other words, the VolaR is the value satisfying

$$\mathrm{P}(\sigma(t) > \mathrm{VolaR}(\alpha)) = \alpha, \tag{12}$$

which is nothing else than the quantile at the $1-\alpha\%$ (on the right-tail) of the log-normal distribution. For instance, when $\alpha = 0.05$ the VolaR is set to 0.0138 (FSV) and 0.0165 (RFSV), which means that the models assign a probability of 5% to the event that the volatility is above 21.91% and 26.19%, respectively on annual basis. When $\alpha = 0.01$ the VolaR is set to 0.0205 (FSV) and 0.0298 (RFSV), which means that the models assign a probability of 1% to the event that the volatility is above 32.54% and 47.31%, respectively on annual basis.

4. Conclusion

This paper analyzed the properties of a class of processes that posses the mean reverting property, which is suitable to model many financial and macroeconomic variables. We computed the variance of the fOU process and derived the probability for its supremum. We considered three examples of the fOU model in the context of stochastic volatility under fractionality. In particular, we looked at FSV model of Comte and Renault (1998), the RFSV of Gatheral et al. (2018), and the rBergomi model introduced in Bayer et al. (2016). The range of applicability of the results of the present paper is rather wide. From a macro-prudential perspective, society relies on the stability of the financial sector. The recent financial crisis led to recession and sovereign debt crises and highlighted the strong impact that risky rates have on the financial stability. Central banks, financial institutions, risk managers as well as most of the agents operating in the financial market need information on the maximum value that volatility (or interest rates) can reach, in order to manage their risks, to hedge financial assets and to construct portfolios of bonds and equities.

Appendix A. Proof of Proposition 1

Proof. In order to derive the theorem, we use the following two results on the fractional Brownian motion established in Cheridito et al. (2003).

i) Let $B^H(t) = \{t \in \mathbb{R}\}$ be a fractional Brownian motion with Hurst parameter $H \in (0, 1)$. Let $-\infty \le a \le \infty$ and $\lambda, \eta > 0$. Then for almost all $\omega \in \Omega$ and for all $t > a$,

$$\int_a^t e^{\lambda u} dB^H(u) = e^{\lambda t} B^H(t) - e^{\lambda a} B^H(a) - \lambda \int_a^t e^{\lambda u} B^H(u) du. \tag{13}$$

Hence, the variance $\varsigma(t) := \mathbb{V}ar[X^H(t)]$ of the fOU process is

$$\begin{aligned}
\varsigma(t) &= \mathbb{E}\left([\eta e^{-\theta t} \int_0^t e^{\theta u} dB^H(u)]^2 \right) \\
&= \eta^2 e^{-2\theta t} \mathbb{E}\left([e^{\theta t} B^H(t) - \theta \int_0^t e^{\theta u} B^H(u) du]^2 \right) \quad \text{by i)} \\
&= \eta^2 e^{-2\theta t} \Bigg(e^{2\theta t} \mathbb{E}[B^H(t)]^2 - 2e^{\theta t} \theta \int_0^t e^{\theta u} \mathbb{E}[B^H(t) B^H(u)] du \\
&\quad + \theta^2 \mathbb{E}\left[\int_0^t e^{\theta u} B^H(u) du \int_0^t e^{\theta v} B^H(v) dv \right] \Bigg) \\
&= \eta^2 t^{2H} - \theta \eta^2 e^{-\theta t} \int_0^t e^{\theta u} (t^{2H} + u^{2H} - |t-u|^{2H}) du \\
&\quad + \eta^2 e^{-2\theta t} \theta^2 \int_0^t \int_0^t e^{\theta u} e^{\theta v} \mathbb{E}[B^H(u) B^H(v)] du dv \\
&= \eta^2 t^{2H} - \theta \eta^2 e^{-\theta t} \int_0^t e^{\theta u} (t^{2H} + u^{2H} - |t-u|^{2H}) du \\
&\quad + \theta^2 \eta^2 e^{-2\theta t} \frac{1}{2} \int_0^t \int_0^t e^{\theta u} e^{\theta v} (u^{2H} + v^{2H} - |u-v|^{2H}) du dv.
\end{aligned} \tag{14}$$

□

Appendix B. Proof of Proposition 2

Proof. First, we recall a result provided in Nourdin (2012).

i) Let $X = \{X(t), t \in [0, 1]\}$ be a centered and continuous Gaussian process. Set $\zeta^2 = \sup_{t \in [0,1]} \mathbb{V}ar[X(t)]$. Set $\xi = \mathbb{E}[\sup_{u \in [0,1]} X(u)]$ finite. Then, for all $x > \xi$

$$\mathbb{P}\left(\sup_{u \in [0,1]} X(u) \ge x \right) \le e^{-\frac{(x-\xi)^2}{2\zeta^2}}. \tag{15}$$

Eq. (15) shows that the supremum of a Gaussian process roughly behaves like a Gaussian variable with variance equal to the largest variance achieved by the entire process. Based on this result, we now derive an expression for the probability for the supremum of the fOU process. In order to prove Theorem 2, note that for $x > 0$ and a constant $c > 0$ one has

$$\int_x^\infty e^{-\frac{y^2}{2c}} dy \le \frac{1}{x} \int_x^\infty y e^{-\frac{y^2}{2c}} dy = \frac{k}{c} e^{-\frac{x^2}{2c}},$$

from which we deduce that $\lim_{x\to\infty} x^{-2}\log\int_x^\infty e^{-\frac{y^2}{2c}}dy = -\frac{1}{2k}$.

Notice that when $t = 1$

$$\frac{1}{\sqrt{2\pi\,\mathbb{V}ar[X^H(1)]}}\int_x^\infty e^{-\frac{y^2}{2\mathbb{V}ar[X^H(1)]}}dy = \mathbb{P}(X^H(1)\geq x) \leq \mathbb{P}(M^H(1)\geq x),$$

where $\mathbb{V}ar[X^H(1)]$ for the fOU is defined in Proposition 1. This implies that

$$\liminf_{x\to\infty} x^{-2}\log\mathbb{P}(M^H(1)\geq x) \geq -\frac{1}{2\mathbb{V}ar[X^H(1)]}. \tag{16}$$

Furthermore, Eq. (15) implies that when x is large enough

$$\log\mathbb{P}(M^H(1)\geq x) \leq -\frac{(x-\mathbb{E}[M^H(1)])^2}{2\sup_{t\in[0,1]}\mathbb{V}ar[M^H(1)]} \leq -\frac{(x-\mathbb{E}[M^H(1)])^2}{2\mathbb{V}ar[X^H(1)]},$$

in turn giving that

$$\limsup_{x\to\infty} x^{-2}\log\mathbb{P}(M^H(1)\geq x) \leq -\frac{1}{2\mathbb{V}ar[X^H(1)]}. \tag{17}$$

Combining (16) and (17) completes the proof. □

References

Andersen, T.G., Bollerslev, T., Diebold, F.X., Ebens, H., 2001a. The distribution of realized stock return volatility. J. Financial Econ. 61 (1), 43–76.

Andersen, T.G., Bollerslev, T., Diebold, F.X., Labys, P., 2001b. The distribution of realized exchange rate volatility. J. Am. Stat. Assoc. 96 (453), 42–55.

Andersen, T.G., Bollerslev, T., Diebold, F.X., Labys, P., 2003. Modeling and forecasting realized volatility. Econometrica 71 (2), 579–625.

Avellaneda, M., Lee, J., 2010. Statistical arbitrage in the U.S. equity market. Quant. Finance 10, 761–778.

Barndorff-Nielsen, O.E., Shephard, N., 2002a. Econometric analysis of realized volatility and its use in estimating stochastic volatility models. J. R. Stat. Soc. Ser. B (Stat. Methodol.) 64 (2), 253–280.

Barndorff-Nielsen, O.E., Shephard, N., 2002b. Estimating quadratic variation using realized variance. J. Appl. Econom. 17 (5), 457–477.

Bayer, C., Friz, P., Gatheral, J., 2016. Pricing under rough volatility. Quant. Finance 16 (16), 887–904.

Bennedsen, M., Lunde, A., Pakkanen, M. S., 2016. Decoupling the short-and long-term behavior of stochastic volatility. arXiv:1610.00332v1.

Bergomi, L., 2005. Smile dynamics. Risk 67–73.

Bernard, C., Jiang, X., Wang, R., 2014. Risk aggregation with dependence uncertainty. Insurance Math. Econ. 54, 93–108.

Bernard, C., Vanduffel, S., 2015. A new approach to assessing model risk in high dimensions. J. Banking Finance 58, 166–178.

Bjork, T., Hyll, M., 2000. Fractional Ornstein–Uhlenbeck Process. Stockholm School of Economics. Unpublished Manuscript

Brigo, D., Mercurio, F., 2001. A deterministic shift extension of analytically tractable and time homogeneous short rate models. Finance Stochast. 5 (3), 369–387.

Caporin, M., Rossi, E., Santucci de Magistris, P., 2017. Chasing volatility: a persistent multiplicative error model with jumps. J. Econom. 198 (1), 122–145.

Chen, Y.-H., Tu, A.H., 2013. Interest rate risk management and the mix of fixed and floating rate deb. J. Banking Finance 27, 514–528.

Cheridito, P., Kawaguchi, H., Maejima, M., 2003. Fractional Ornstein–Uhlenbeck processes. Electron. J. Probab. 8 (3), 1–14.

Comte, F., Renault, E., 1998. Long memory in continuous-time stochastic volatility models. Math. Finance 8 (4), 291–323.

Corsi, F., 2009. A simple approximate long-memory model of realized volatility. J. Financial Econom. 7, 174–196.

Corsi, F., Renò, R., 2012. Discrete-time volatility forecasting with persistent leverage effect and the link with continuous-time volatility modeling. J. Bus. Econ. Stat. 30, 368–380.

Cox, J.C., Ingersoll, J.E., Ross, S., 1985. A theory of the term structure of interest rates. Econometrica 53 (2), 385–407.

Delves, L., Lyness, J., 1967. A numerical method for locating the zeros of an analytic function. Math. Comput. 21 (100), 543–560.

Embrechts, P., Puccetti, G., 2006a. Bounds for functions of dependent risks. Finance Stochast. 10 (3), 341–352.

Embrechts, P., Puccetti, G., 2006b. Bounds for functions of multivariate risks. J. Multivariate Anal. 97 (2), 526–547.

Engle, R.F., Patton, A., 2001. What is a good volatility model? Quant. Finance 1, 237–245.

Filipovic, D., 2007. Energy Risk: Valuing and Managing Energy Derivative, 2nd ed McGraw Hill, New York.

Gatheral, J., Jaisson, T., Rosenbaum, M., 2018. Volatility is rough. Quant. Finance 18 (6), 933–949.

Gnedenko, B.V., 1943. Sur la distribution limite du terme maximum d'une série aléatoire. Ann. Math. 44, 423–453.

Gouriéroux, C., Monfort, A., Renault, E., 1993. Indirect inference. J. Appl. Econom. 8, 85–118.

Heston, S.L., 1993. A closed-form solution for options with stochastic volatility with applications to bond and currency options. Rev. Financial Stud. 6, 327–343.

Hull, J., White, A., 1990. Pricing interest rate derivative securities. Rev. Financial Stud. 3, 573–592.

Jacquier, A., Pakkanen, M.S., Stone, H., 2018. Pathwise large deviations for the rough Bergomi model. J. Appl. Probab. 55 (4), 1078–1092.

Kaeck, A., Alexander, C., 2012. Volatility dynamics for the S&P 500: further evidence from non-affine, multi-factor jump diffusions. J. Banking Finance 36 (11), 3110–3121.

Kaeck, A., Alexander, C., 2013. Continuous-time VIX dynamics: on the role of stochastic volatility of volatility. Int. Rev. Financial Anal. 28, 46–56.

Kolmogorov, A., 1940. Wienersche spiralen und einige andere interessante kurven im hilbertschen raum. Comptes Rendus (Doklady) de l'AcadÃ©mie des Sciences de l'URSS (N.S.) 26, 115–118.

Kou, S., Peng, X., 2016. On the measurement of economic tail risk. Oper. Res. 64 (5), 1056–1072.

Kroese, D.P., Botev, Z.I., 2015. Spatial process simulation. In: Stochastic Geometry, Spatial Statistics and Random Fields. Springer, pp. 369–404.

Kwona, O.K., 2007. Mean reversion level extensions of time homogeneous affine term structure models. Appl. Math. Finance 14, 291–302.

Lai, K.S., 2004. On structural shifts and stationarity of the ex-ante real interest rate. Int. Rev. Econ. Finance 13 (2), 217–228.

Liu, L.Y., Patton, A.J., Sheppard, K., 2015. Does anything beat 5-minute RV? a comparison of realized measures across multiple asset classes. J. Econom. 187 (1), 293–311.

Mandelbrot, B., Van Ness, J., 1968. Fractional brownian motions, fractional noises and applications. SIAM Rev. 10, 422–437.

Nourdin, I., 2012. Selected Aspects of Fractional Brownian Motion. Bocconi University Press. Springer-Verlag Italia, Milan.

Rossi, E., Santucci de Magistris, P., 2014. Estimation of long memory in integrated variance. Econom. Rev. 33 (7), 785–814.

Rossi, E., Santucci de Magistris, P., 2018. Indirect inference with time series observed with error. J. Appl. Econom. 33 (6), 874–897.

Sauri, O., 2019. Pathwise decompositions of Brownian semistationary processes. Theory Probab. Appl. 64 (1), 78–102.

Tan, J., 1997. Principal component analysis and portfolio optimization. Math. Finance 7, 95–105.

Vasicek, O., 1977. An equilibrium characterisation of the term structure. J. Financial Econ. 5, 177–188.